STAR FORMATION HISTORY AND EXTINCTION IN NGC 206

Todor Veltchev

Institute of Astronomy
Bulgarian Academy of Sciences, Bulgaria

and

P. Nedialkov and G. R. Ivanov

Department of Astronomy
University of Sofia, Bulgaria

RESUMEN

La historia de la formación estelar en la superasociación NGC 206 en M31 se ha estudiado utilizando la mejor fotometría obtenida hasta el momento (Hunter et al. 1996). La comparación entre los cocientes de estrellas azules y rojas teóricos y observacionales sugiere la existencia de brotes de formación estelar secuenciales. El último de los brotes de formación estelar parece haber tenido una mayor eficiencia en comparación con el resto. La correlación espacial entre diferentes indicadores de la formación estelar y de la edad (candidatos a Cefeidas, supergigantes rojas y estrellas en la secuencia principal) sugiere que la formación estelar ha sido inducida por ondas de choque. El estudio de la extinción en NGC 206 relaciona a dos asociaciones OB (descritas por Efremov, Ivanov, & Nikolov 1987) con regiones de extinción pequeña y casi constante. Esto sugiere que la formación estelar violenta ocurrida en esta superasociación ha llevado al completo agotamiento del material en la nube primordial.

ABSTRACT

Using the state-of-the-art photometry of NGC 206 obtained by Hunter et al. (1996) the history of the star formation in this superassociation in M31 is studied. The comparison of the observational and the theoretical blue-to-red stars ratios (B/R) suggests that probably three sequential starbursts have occurred, with an increased star formation efficiency during the last one. The conjecture about generation and reflection of shock waves as a trigger of star formation is supported by the calculated spatial correlation between Cepheid candidates, red supergiants and main sequence stars of different mass range. The extinction study of NGC 206 relates two OB associations outlined by Efremov, Efremov, Ivanov, & Nikolov (1987) with regions of small and almost constant extinction. That confirms the assumption of violent star formation which have led to an exhaustion of the natal cloud material.

Key words: **INTERSTELLAR MEDIUM: EXTINCTION — STARS: B/R RATIO — STARS: FORMATION — STARS: REDDENING**

1. INTRODUCTION

The history of the star formation in stellar groupings of different size is an issue which has been recently subject of intensive studies. The knowledge of this history is of crucial significance for determining some major characteristics of the stellar associations like age, spatial structure, amount of gas and dust, and for testing of the possible mecha-

13

nisms of star formation. For this purpose powerful methods like population synthesis (e.g., Tosi et al. 1991) and maximum likelyhood method (e.g., Hernandez, Valls-Gabaud, & Gilmore 1998) have been elaborated. A simpler but in many cases effective approach to the problem is the calculation of the blue-to-red stars ratio (B/R ratio) which is used in the present paper.

The stellar complex NGC 206 (OB 78 in the catalogue of van den Bergh 1964) in the Andromeda galaxy is an appropriate object for studying the star formation history because of its size, its place in a region of lower density of the neutral hydrogen (Brinks & Bajaja 1986) and of the large amount of young stars. The latter evidence testifies for a strongly increased star formation efficiency. Chernin, Efremov, & Voinovich (1995) call such complexes 'superassociations' and hereafter, we adopt this term for NGC 206. It reveals distinct substructure of classic associations as they were outlined by Efremov et al. (1987) and Battinelli (1991). The stellar population in NGC 206 is well studied by different authors (Massey, Armandroff, & Conti 1986, hereafter MAC; Odewahn 1987; Efremov 1989; Hunter et al. 1996; Magnier et al. 1997). Hunter et al. (1996, hereafter HBOL) provided the deepest up-to-date photometry of OB 78 by the *Hubble Space Telescope (HST)* which gives the opportunity for extensive investigations of different stellar generations and the distribution of the absorbing matter, and also for checking the theoretical models of star formation and stellar evolution.

2. PRELIMINARY PROCEDURES

2.1. *Differential Dereddening*

Our study is based on the CCD photometry of HBOL of more than 15,000 stars located in NGC 206. The images were obtained by the Wide Field Planetary Camera (WFPC2) of *HST* through the filters F336W, F555W, and F814W (hereafter designated as UVI_{HST}). The correct estimation of the differential reddening faces two main difficulties: 1) the transformations between the standard (Johnson's UBV) and the *HST* system, and 2) the problems of measuring the brightness of the individual stars when a blending occurs. To overcome the problems, we juxtaposed carefully the *HST* data and the UBV photometry of MAC, which covers a region containing the whole mosaic of 4 WFPC2 images. The procedures of dereddening and distinguishing of the luminosity classes (supergiants and main sequence stars) are intertwined. On the one hand, the reddenings have to be known in order to determine the luminosities and the unreddened colors. On the other hand, if no spectral information is available, one needs the unreddened sequences (with a possible noticeable shift on the two-color diagram) for both

classes to obtain the appropriate reddening estimations.

Fortunately, we have in common 94 nonblended stars (with $\sigma_{E(B-V)} < 0.1$) from both the samples and 44 of them are supergiants easily recognized on the HRD diagram after applying the conventional Q-method. Additional data for 3 common red supergiants are available from Massey (1998) as well. Because of the different limiting magnitudes of the samples MAC and HBOL the supergiants cover a wider range of colors which is crucial for the transformation of the photometric system. To determine the reddening in the UBV and UVI_{HST} filters without contradiction, we adopted for both the unreddening procedures $R_V = A_V/E(B - V) = 3.1$ and a slope $E(U - B)/E(B - V) = 0.68$ based on the extinction curve of Cardelli, Clayton, & Mathis (1989). Then the tabulations of Holtzman et al. (1995) were used for determination of the reddenings in *HST* colors of those common stars for which $E(B - V)$ and Q-index (or the spectral type) are previously known. To transform the standard Johnson's $(U - V)_0$ and $(B - V)_0$ colors to the $(U - V)_0$ and $(V - I)_0$ colors in *HST* system the following approximations were derived (see Figure 1)

$$(U - V)_{0,HST} = 0.353_{\pm 0.085} + 1.906_{\pm 0.098}(U - V)_{0,J},$$

$$(U - V)_{0,J} < 0.14$$

$$(V - I)_{0,HST} = 0.019_{\pm 0.024} + 1.060_{\pm 0.172}(B - V)_{0,J},$$

$$(B - V)_{0,J} < 0.85$$

$$(U - V)_{0,HST} = 0.529_{\pm 0.594} + 0.713_{\pm 0.188}(U - V)_{0,J},$$

$$(U - V)_{0,J} > 0.14$$

$$(V - I)_{0,HST} = -0.861_{\pm 0.986} + 2.112_{\pm 0.658}(B - V)_{0,J},$$

$$(B - V)_{0,J} > 0.85$$

The larger errors in the second group of equations are due to the lack of statistics for redder supergiants. From these equations, we obtained also the shifted unreddened sequence for supergiants and the top of the unreddened sequence for dwarfs.

The initial sample consists of 2711 stars (predominantly from the main sequence) with UVI photometry and it is practically free from background contamination (see next section). In order to determine the individual reddening of each star we constructed grids of reddening lines (both for supergiants and main sequence stars) and lines of constant $E(B - V)$ on the two-color diagram (Figure 2). A few hundred stars and one half of the unresolved clusters in MAC
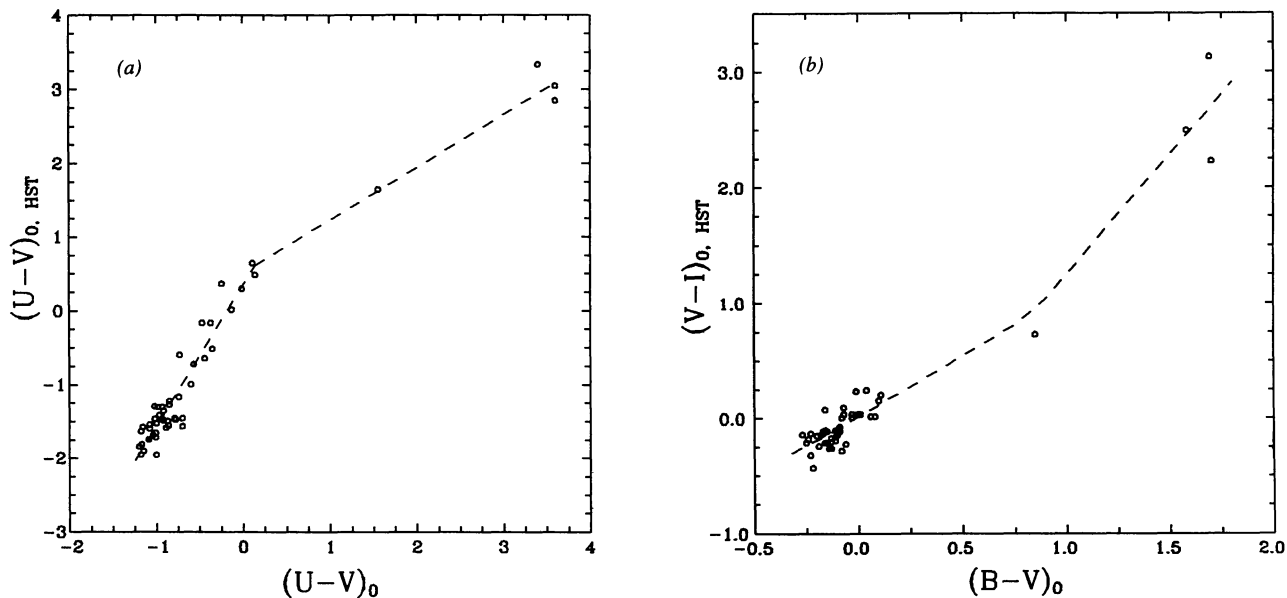
Fig. 1. The transformations of the standard Johnson's colors: (a) $(U - V)_0$, and (b) $(B - V)_0$ to the corresponding colors of the HST system.
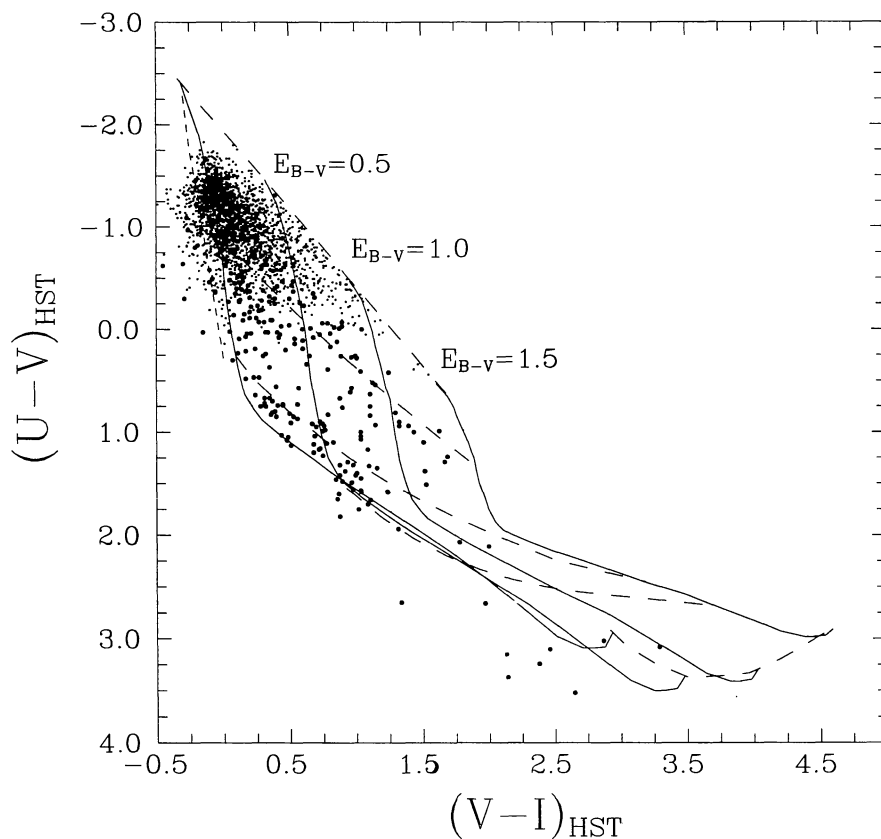
Fig. 2. The two-color diagram with differential reddening grid for supergiants according to the derived zero absorption line and the tabulations of Holztman et al. (1995). The lines of constant $E(B - V)$ are solid (with the corresponding value above) and the reddening lines are dashed. The supergiants are depicted by larger dots (in comparison with the MS stars).

lay above the reddening line for the bluest O stars. This phenomenon might be explained with errors of photometry, different slope of the reddening line and images of nonstellar objects behind the disk of M31. Since the incorrectly measured colors could produce incorrect reddening values, the stars above the reddening line for the bluest O stars and those with extremely negative reddening were excluded from the initial sample. All the stars were dereddened to both luminosity class sequences (supergiants and dwarfs) on the two-color diagram and their images were plotted on a CM-diagram. Considering the transformed evolutionary tracks a color-luminosity criterion was derived for distinguishing the supergiants from the main sequence stars

$$(U - V)_0 = 0.109 + 0.110 \ M_V - 1.61 \times 10^{-2} \ M_V^2$$

$$-8.65 \times 10^{-3} \ M_V^3 - 7.71 \times 10^{-4} \ M_V^4 \ .$$

Special adjustments were made for dereddening the supergiants of 'intermediate' color. As it is evident from Figure 2, in this case the reddening line is running close with the zero-absorption line. The reddenings of such stars were determined as the average value of their neighbors' reddenings within 10 arcsec. Finally, we obtained the reddening values in terms of $E(B - V)$ for 1984 main sequence stars and 366 supergiants. Their distributions are presented in Figure 3. Later on, we have used these values to study the extinction within NGC 206.

2.2. Transformation of the Theoretical Tracks and Isochrones

We have used the theoretical tracks and isochrones of the Geneva group calculated with 'normal' mass loss rate and with overshooting for initial stellar masses between 4 and 60 $M_\odot$ (Schaerer et al. 1993). The preliminary transformation from $\log T_{eff}$ to Johnson's color $B - V$ and the calculation of the bolometric correction were performed according to the empirical formulae of Flower (1996). The transition to Johnson's color $U - V$ was accomplished through an interpolation based on numerous studies and suggested by Straizys (1977). Further, we used the transformation equations from the previous paragraph. These do not contradict neither the observed trends for the supergiants nor the predicted synthetic transformation (Holtzman et al. 1995). We calculated the average metallicity in the superassociation using the fit for metallicity gradient in M31 of Issa, MacLaren, & Wolfendale (1990). For the galactocentric distance of NGC 206, it turns out to be almost twice higher than the solar one and therefore, the value $Z = 0.04$ was adopted.
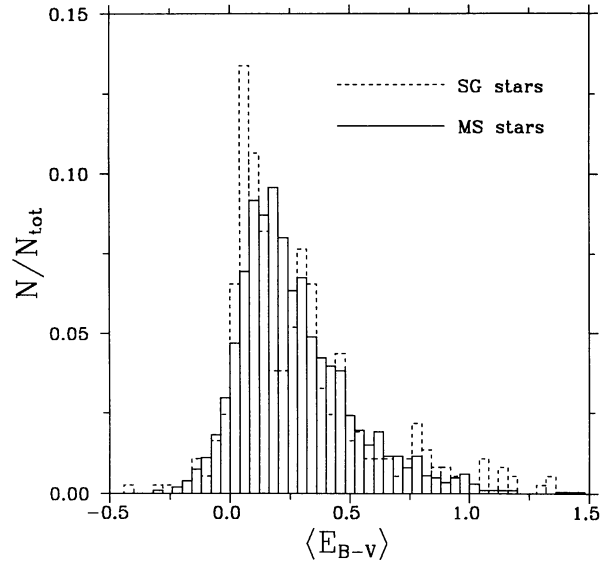

Fig. 3. The distributions of the reddenings in terms of $E(B - V)$ for 1984 main sequence stars and 366 supergiants within NGC 206.

3. DETERMINATION OF THE B/R RATIO

3.1. Observational Estimation

In order to decrease the errors we have counted only the stars which lay over the theoretical track for 7 $M_\odot$ on the CM-diagram. With the photometry of HBOL this track corresponds to an incompleteness level of 10 – 15% and it avoids the area of significant background contamination. Now, the first step to determine the B/R ratio is to define correctly the criterion for distinguishing between 'blue' and 'red' stars. In terms of color, one usually accepts as 'blue' stars those with negative values of $(B - V)_0$ which approximately corresponds to effective temperatures above 10,000 K and the slowest evolution on the HR diagram (see Langer & Maeder 1995). The 'red boundary' is not fixed strictly in the literature, and we named 'red' those stars with $(B - V)_0 \geq 1.0$ (this criterion is adequate since according to Ratnatunga & Bahcall [1985], the foreground contamination of galaxy dwarfs for this color range and per area of 10 arcmin^2 is negligible). Since the dereddened stars from the sample of HBOL have $(V - I)_0$ colors (in the system of WFPC2) we adopted a criterion in this color: $(V - I)_0 \leq 0.03$ and $(V - I)_0 \geq 1.3$ which are the typical values for supergiants with already mentioned $(B - V)_0$ colors. Because of the limits of the photometry, there is a lack of red supergiants with UVI-colors under the 9 $M_\odot$ track. Therefore, we added to our sample red stars without U color and $1.3 \leq (V - I)_0 \leq 3$ with averaged corrections for

reddening and absorption 0.20 and 0.47 correspondingly (see HBOL). The next step to make is to count the background stars under the accepted criteria and to subtract their number from the sample. For this purpose, we have used the photometry of HBOL of an nearby area of NGC 206 within the same field-of-view. The actual number of background stars of such magnitudes is found to be very small. The color and the magnitude of those stars were also corrected with the averaged values of the color excess and absorption. Finally, the sample was divided in bins with different value of the incompleteness factor (see Table 4 of HBOL) and the number of stars in each one was corrected accordingly. The B/R ratio was calculated taking into account the errors of measurement in V and $V - I$ (See § 4).

3.2. A Theoretical Approach

The B/R ratio could be a very sensitive test for the theory of stellar evolution and for the physical processes implemented in the stellar models like mass loss due to different mechanisms, semiconvection and overshooting (for an overview see Langer & Maeder 1995). The comparison between their observational and theoretical values gives an important information about the history of star formation. Here we present a simple method to obtain the B/R ratio from the theoretical isochrones and under certain assumptions about the star formation rate.

Let us define the upper mass limit M_{up} and the lower mass limit M_{down} on the isochrone. (These values are the INITIAL masses of a star on the ZAMS) M_{up} could be evaluated on the base of some theoretical assumptions about the upper mass limit of stars which still exists at the given moment of time wherea M_{down} is determined from photometry taking into account the incompleteness level and the background contamination. Let us assume also that the star formation time is very short in comparison with the age of the association, i.e., all N_* stars of some generation were born simultaneously. We accept a constant slope of the initial mass function Γ for all generations of stars within the association. The number of stars N_1 with masses between some M_1 and M_2 values is obviously proportional to the area S_1 in Figure 4, where the continuous curve is the initial spectrum of masses

$$N_1 \propto \int_{M_1}^{M_2} m^{\Gamma - 1}\, dm = \frac{m^\Gamma}{\Gamma} \quad , \qquad (1)$$

where $\Gamma = \gamma + 1$ is the slope of initial mass function and γ is the slope of initial mass spectrum. The coefficient of proportionality here has the meaning of mean density of stellar mass distribution. Now the 'blue' stars are those with masses under $M_{b,down}$
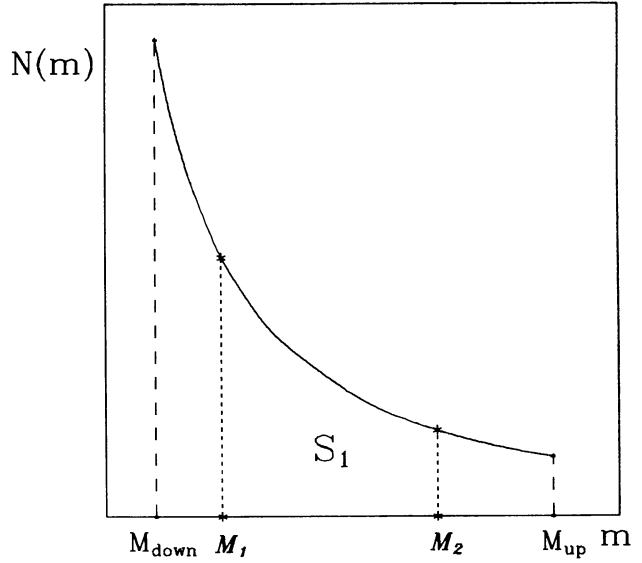

Fig. 4. Toward a determination of the B/R ratio when the initial spectrum of masses is known. The number of stars with masses between M_1 and M_2 is proportional to the area S_1.

and, in case of some earlier isochrones, over $M_{b,up}$; and the 'red' ones are those with masses over $M_{r,down}$ and, in case of some earlier isochrones, under $M_{r,up}$ (see Figures 5a,b). Hence, the B/R ratio resulting from a single starburst is a ratio of integrals

$$\frac{B}{R} = \frac{N_B}{N_R} = \frac{\int_{M_{down}}^{M_{b,down}} m^{\Gamma - 1}\, dm}{\int_{M_{r,down}}^{M_{up}} m^{\Gamma - 1}\, dm} = \frac{M_{B,1}}{M_{R,1}} \quad . \qquad (2)$$

This formula could be easily generalized in case of n different starbursts. In the numerator and in the denominator we will have sums of integrals where each of them is normalized to the number of stars being born during the first burst

$$\frac{N_B}{N_R} = \frac{\sum_{i=1}^{n} A_i\, M_{B,i}}{\sum_{i=1}^{n} A_i\, M_{R,i}} \quad ; \qquad (3)$$

$A_i = N_i/N_*$ are the coefficients of normalization. For instance, if during the second burst twice less stars were born, the value of A_2 would be $1/2$. If the $j-$th generation is so young that no 'red' stars exist then $M_{R,j} = 0$.
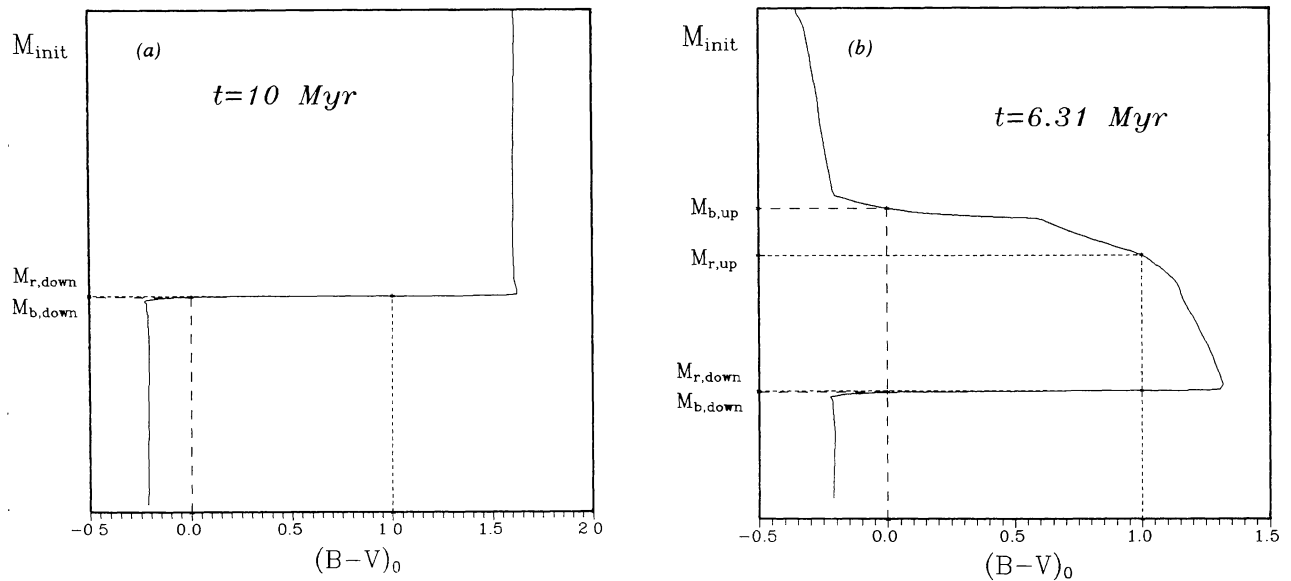
Fig. 5. Determination of the upper and lower mass limit of the 'blue' and 'red' stars from an isochrone presented in plain 'color-initial mass'. The limits M_{down} and M_{up} lie beyond the diagram. (a) In case of a later isochrone only $M_{b,down}$ and $M_{r,down}$ exist. Their values are very close because of the fast transition to the red part of CM-diagram after the exhaustion of hydrogen in the stellar core. $M_{r,up}$ coincides with M_{up}. (b) In case of an earlier isochrone one has to determine all the mass limits of the 'blue' and 'red' stars.

4. MAIN RESULTS

4.1. B/R Ratio, Isochrones and CM-Diagram

The results from the observational estimation of the B/R ratio are listed in Table 1. With σ_V, σ_{V-I} we denote the observational errors according to HBOL and $\sigma = (\sigma_V^2 + \sigma_{V-I}^2)^{0.5}$ is the total error. The sign 'plus' ('minus') means that the stars within distance from the track are included in (excluded from) the calculation. The range of values of B/R is obviously too large and this is a consequence of the relatively high observational uncertainties. If we restrict the results only to the uncertainties in V the value of B/R is determined with precision of 14%.

In Figure 6 the observable CM-diagram for stars with UVI-photometry is plotted. The oldest generation in NGC 206 is presented by the Cepheid candidates in and around the instability strip. Five of them were identified in comparison with the works of Baade & Swope (1965) and Gaposhkin (1962), and are listed in Table 2 together with their coordinates in the General Catalogue of Variable Stars (1995).

The position of the Cepheid candidates on the CM-diagram fits approximately the isochrones $\log(t) = 7.5$ and $\log(t) = 7.6$ (where the age t is measured in years) and we take therefore, those values as the age of the first generation of stars in

NGC 206. The best fits of another distinct group give the isochrones $\log(t) = 7.0$ and $\log(t) = 7.1$.

So we applied our theoretical approach for calculation of the B/R ratio assuming two or three sequential starbursts in the star formation history and adopting for the slope of the initial mass function $\Gamma = -1.4 \pm 0.5$ as obtained by HBOL. The results are listed in Table 3. The theoretical B/R ratio is clearly not sensitive to the exact value of Γ but it depends significantly on the number of starbursts. Comparing the results with the observational estimations from Table 1 (despite the uncertainties of the latter due to photometry), we could infer that a scenario with three starbursts is the most probable one. Even more impressive are the results when one assumes that the star formation rate during the last burst was twice higher (see Table 4). In this case, the observed and the predicted B/R ratios coincide within the range of errors of the photometry ($2\sigma_V$) and Γ. Of course, these results delineate only qualitatively the star formation history in NGC 206 but convincingly testify to an increased star formation efficiency during the last burst.

4.2. Correlation Between the Stellar Generations

For estimation of the relation between the various stellar generations we used the correlation technique
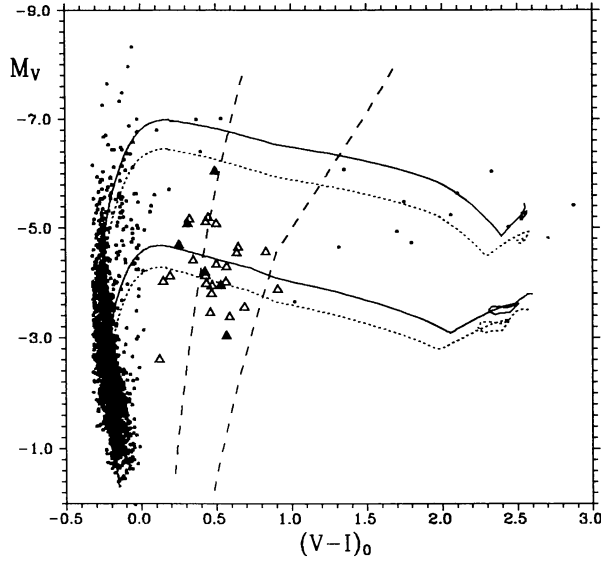
Fig. 6. Stars with *UVI*-photometry on the CM-diagram of NGC 206. The isochrones $\log(t) = 7.6$, $\log(t) = 7.1$ are drawn with short dashed lines, $\log(t) = 7.5$ and $\log(t) = 7.0$ with solid lines and the instability strip with dashed lines. The triangles indicate the Cepheid candidates (with filled triangles is shown the position of the identified objects among them; see text).

of Ivanov (1998). It gives the percentage of spatially associated couples of stars of two different groups by ratios R1 and R5 which correspond to statistical confidence of 99% and 95%, respectively. Another estimator of the correlation between two stellar generations are the ratios of the actual number of associated objects to the expected number from random distributions of both generations. These ratios are denoted by RN5 for statistical confidence of 95% and by RN9 for confidence of 99%. The values R1 $\approx$ 1, R5 $\approx$ 1, and also RN9 $\geq$ 3 and RN5 $\geq$ 5, testify to a strong correlation between two stellar generations. When there are no associated stars between two stellar groups, one obtains R1 $\sim$ 0, R5 $\sim$ 0, RN1 $\leq$ 1, RN5 $\leq$ 1. In all the cases, the stronger criterion is to require statistical confidence of 99%.

The correlation parameters between different stellar groups and generations in NGC 206 are given in Table 5. The best correlation is found between the Cepheid candidates and the populations of intermediate mass MS stars (< 7 and $7 - 12$ $M_\odot$). This correlation is expected, since it is well known that the progenitors of the Cepheids are MS stars between 5 and 12 $M_\odot$. However, most of the Cepheids with periods $> 10^d$ evolved from MS stars with $5 - 7$ $M_\odot$ and, indeed, in this case we have R5 = 0.97. The relatively good correlation between the less massive MS stars with $M < 7$ $M_\odot$ and the red supergiants (RSGs) (with $(V-I)_0 > 1.3$) could be explained with the fact that most of the stars of both the groups

TABLE 2

IDENTIFIED CEPHEIDS IN NGC 206[a]

Design.	Ref.	Type	Period (days)	Coordinates (1950.0)	
72	G 62	δ Cep	10.4609	0 37 45.20	+40 29 11.0
110	G 62	δ Cep	4.900	0 37 45.50	+40 28 53.0
146	G 62	δ Cep	8.0 ?	0 37 46.60	+40 28 27.0
V344-III	BS 65	δ Cep	5.040	0 37 45.61	+40 26 04.3
V342-III	BS 65	Semiregular	....	0 37 41.64	+40 26 53.6

[a] The meaning of the abbreviations is as follows: Desig. = designation of the star in the corresponding work. Ref. = G 62, Gaposhkin (1962); BS 65, Baade & Swope (1965). The stellar type and the period are also given.

TABLE 3

THEORETICAL PREDICTIONS FOR THE B/R RATIO[a]

1st Starburst	2nd Starburst	3rd Starburst	Γ	B/R
7.6	7.1	...	-1.4	6.96
7.6	7.1	...	-1.9	7.15
7.6	7.1	...	-0.9	6.67
7.6	7.0	...	-1.4	6.74
7.6	7.0	...	-1.9	7.25
7.5	7.1	...	-1.4	6.07
7.5	7.0	...	-1.4	6.01
7.6	7.1	6.6	-1.4	18.71
7.6	7.0	6.6	-1.4	16.56
7.6	7.1	6.5	-1.4	16.57
7.5	7.1	6.6	-1.4	14.68
7.5	7.0	6.6	-1.4	13.55
7.5	7.1	6.5	-1.4	13.55

[a] In the first three columns is given the time since the sequential starbursts, in units of $\log(t)$, with t in years.

TABLE 4

THEORETICAL PREDICTIONS FOR THE B/R RATIO[a]

1st Starburst	2nd Starburst	3rd Starburst	Γ	B/R
7.6	7.1	6.6	-0.9	34.30
7.6	7.1	6.6	-1.4	30.46
7.6	7.1	6.6	-1.9	27.97
7.6	7.1	6.5	-1.4	30.48
7.6	7.0	6.6	-1.4	26.39
7.6	7.0	6.6	-1.9	25.97
7.5	7.1	6.6	-1.4	23.30
7.5	7.1	6.5	-1.4	23.32
7.5	7.0	6.6	-1.4	21.08

[a] The star formation rate of the last burst (the third one) is artificially increased twice.

belong to one and the same generation. Significant for the study of the star formation history are the correlations between the MS stars of different mass range. All of them with masses greater than 12 $M_\odot$ are extremely young and their eventual correlation with stars of an older generation could show the spatial domain where the last starburst took place. The relatively good correlation between the most massive MS stars and the Cepheid candidates indicates that the youngest stars in NGC 206 were born not far away from the areas of the first starburst. On the other side, their formation occurred far in space from the position of the second stellar generation rep-

resented partly by the RSGs and some MS stars with masses $7 - 12$ $M_\odot$ (see Table 5). Actually, Efremov (1989) had noted already the different locations of the Cepheids and the OB stars in NGC 206, so we can imagine two types of spatial groupings: those containing the oldest and the youngest stars in the superassociation and the others consisting of stars of intermediate age. This conclusion has an interesting link with the star formation scenario in NGC 206 suggested by Chernin et al. (1995). They supposed at least two sequential starbursts: an 'ordinary' first one (in terms of star formation mechanisms) and a second one caused by propagation and reflection of shock

TABLE 5

CORRELATION COEFFICIENTS BETWEEN
DIFFERENT GROUPS OF STARS[a]

Group of Stars	R5	R9	RN5	RN9	Correlation
msl_7 — ceph	0.97	0.59	36.0	22.0	very strong
ms7_12 — ceph	0.86	0.49	32.0	18.0	very strong
msl_7 — RSGs	0.59	0.38	3.9	2.9	relat. good
msg_12 — ceph	0.57	0.38	4.2	2.8	relat. good
msg_12 — ms7_12	0.56	0.31	3.9	2.2	weak
msg_12 — msl_7	0.52	0.27	3.8	2.0	weak
ms7_12 — RSGs	0.52	0.23	2.8	1.3	weak
msg_12 — RSGs	0.29	0.10	0.7	0.2	no
ms7_12 — msl_7	0.20	0.09	0.4	0.2	no

[a] The meaning of the abbreviations is as follows: msl_7 = MS stars with mass less than 7 $M_\odot$; ms7_12 = MS stars with masses between 7 and 12 $M_\odot$; msg_12 = MS stars with masses greater than 12 $M_\odot$; ceph = Cepheids; RSGs = red supergiants.

fronts. According to this scenario the superassociation was divided into two separate domains of secondary star formation ('associations') in which the reflected fronts propagated after they had met. In the meantime, the first generation stars evolved and so the extremely young stars which formation was triggered by the reflected fronts and the Cepheids are situated close in space.

4.3. Extinction in NGC 206

HBOL adopted a single reddening estimation for all the stars in NGC 206, $E(B-V) = 0.14$ as not a bad approximation of reality. Combining photometric and spectroscopic studies of NGC 206, Massey et al. (1995) found that here the quantity $q_r = E(U-B)/E(B-V)$ amounts to 0.43 ± 0.07, in discrepancy with the expected value of 0.72. They concluded that this low value is characteristic of the interstellar extinction in the M31 galaxy. However, we could not accept it since the tabulations of Holtzman et al. (1995) are based on the value $q_r = 0.68$ (Cardelli et al. 1989) and hence $q_r = 0.43$ would affect the HST color in an unpredictable way. In the work of Massey et al. (1995) the average $E(B-V)$ lies between 0.12 ($q_r = 0.5$) and 0.16 ($q_r = 0.72$). These values correspond nicely to the maxima in the distribution of excesses shown in Figure 3. Such result would be obtained if one assumes that the reddening of the most clumped region on the two-color diagram is equal to the mean excess. That is the typical single dereddening procedure when all the stars are dereddened with one and the same reddening vector.

The determined reddenings are representative for the extinction of a few crowded groups of very massive MS stars. These are located mainly within two classic OB associations (Efremov et al. 1987) with a mean size of 80 pc which is believed to be the same in nearby galaxies (Ivanov 1996). The average values of $E(B-V) = 0.27 \pm 0.01$ (for MS stars) and 0.28 ± 0.02 (for supergiants) are identical and they would not be strongly affected if the 'negative' excesses are excluded (the positive shift is only 0.02 mag). In order to study the variance of the extinction, we divided the area in square cells (bins) of constant width and calculated the correlation coefficient between the mean excesses in neighboring bins ('neighboring' are called two bins with a common side, each of them containing at least 1 star). We let the size of the cells to vary from 2 up to 20 arcsec changing also the zero point of the grid and found a constant increasing of the correlation reaching a maximum of 0.50 ± 0.06 at 18 arcsec, i.e., about 70 pc at the distance of M31 (see Figure 7). Since the number of the cells is decreasing strongly as the bin size grows the study of correlations in the excesses is limited.

The calculated weak correlation confirms the large variance of the extinction even from star to star. This picture of the extinction distribution is retained until the bin size approximates the dimensions of the real associations. Due to the asymmetric shape of the excesses' distributions the median values of $E(B-V) \sim 0.20$ are lower than the average values. The isocontours connecting the median values of the extinction clearly distinguish the regions with low extinction from those with a high one (see Figure 8) following approximately the boundaries of the classic OB associations. The extinction study of the two outlined associations shows a shift of the median values at 0.17 which is closer to the distribution
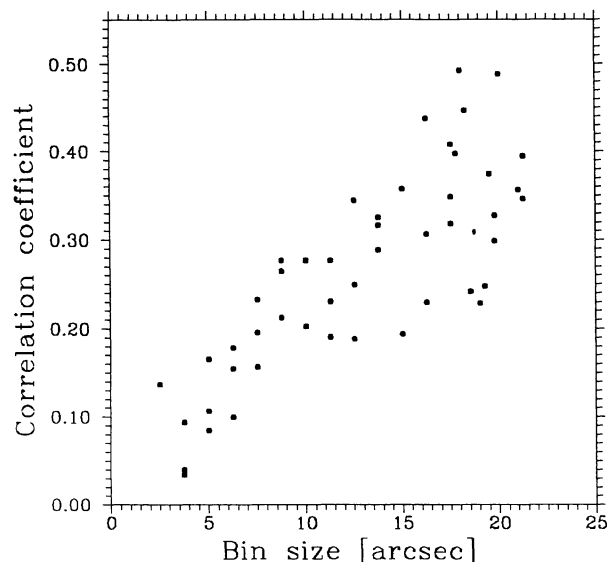
Fig. 7. The correlation coefficient of the excesses in neighboring bins as a function of the bin size. Different values for one and the same bin size are obtained changing the zero point of the grid.
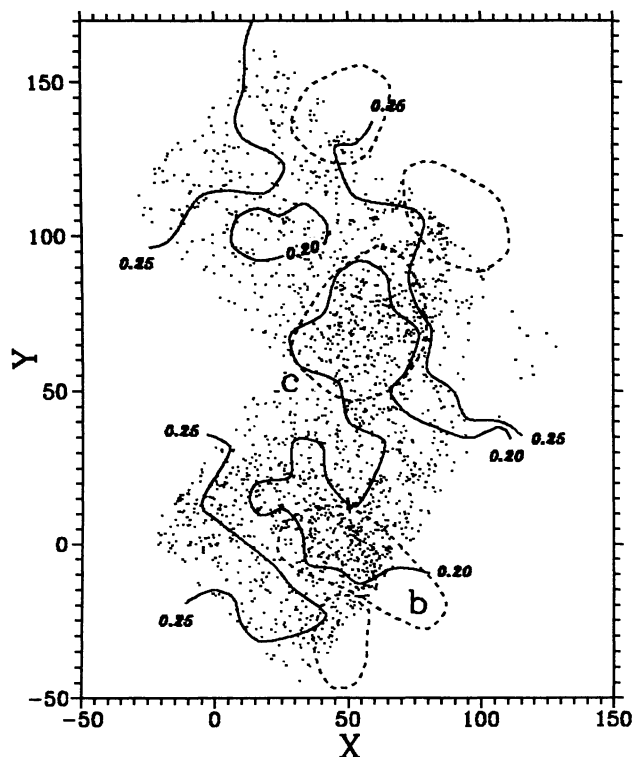

Fig. 8. The boundaries of the OB associations according to Efremov et al. (1987) (dashed lines) superimposed on the NGC 206 map. The isocontours of median extinction (solid lines) of value $E(B - V) = 0.20$ outline approximately the associations 'b' and 'c'. North is to the top of the picture. For a zero-point of the XY coordinate system we have chosen the WR star #82 from MAC.

maximum at 0.12 and is due to its more symmetrical shape. The extinction minimum within the superassociation OB 78 is confirmed also by considering the integrated H I contours of the density maps (Brinks & Bajaja 1986), where a prominent 'hole' in this area is detected. We emphasize also that the 'true' $E(B - V)$ would be considerably smaller since the above mentioned extinction values reflect the total reddening from M31 and from our Galaxy. Taking into account the foreground reddening from the Milky Way $E(B - V) = 0.08$ (Burstein & Heiles 1984), one obtains an almost vanishing internal extinction in NGC 206. Thus we confirm the expectation of HBOL that the massive stars had swept the natal cloud material in areas of star formation with increased efficiency.

5. CONCLUSIONS

By the means of the B/R ratio and correlation techniques we have investigated the history of the star formation in NGC 206. The star formation rate as a function of time was simplified and represented as a sequence of discontinuous bursts of short duration (in comparison with the age of the object). The juxtaposing of the observed and the theoretical B/R ratios shows that three starbursts, with increased efficiency for the last one, are the most probable scenario. Better agreement could be obtained describing the star formation rate with a continuous function of time and using a more powerful method. The 'three bursts scenario' is confirmed also by applying a correlation technique between the Cepheid candidates, RSGs, and groups of MS stars in different mass range. Two distinct OB associations containing stars of the first generation and young massive stars are outlined, which supports the suggestion for reflected shock waves as a trigger of star formation in NGC 206. These two associations could be distinguished also by the means of extinction study. They are depicted as areas of small and almost constant extinction. If Valentijn's (1990) claim of a high opacity of the spiral disks (including that of M31) is correct, that testifies to a very high star formation efficiency in NGC 206 which could lead to a full sweeping of natal material. Following this line of thought, we may surmise that the classic OB associations are indeed locations in the spiral arms with not too high optical thickness and enough high star formation efficiency so that the young massive stars could be observed.

REFERENCES

Baade, W., & Swope, H. 1965, AJ, 70, 212

Battinelli, P. 1991, Mem.Soc.Astr.Ital., 62, 959

Brinks, E., & Bajaja, E. 1986, A&A, 169, 14

Burstein, D., & Heiles, C., 1984, ApJS, 54, 33

Cardelli, J., Clayton, G., & Mathis, J. 1989, ApJ, 345, 245

Chernin, A., Efremov, Yu., & Voinovich, P. 1995, MN-RAS, 275, 313

Efremov, Yu. 1989, in Origin of Star Formation in Galaxies (Moskva: Nauka, in Russian), 104

Efremov, Yu., Ivanov, G., & Nikolov, N. 1987, Ap&SS, 135, 119

Flower, P. 1996, ApJ, 469, 355

Gaposhkin, S. 1962, AJ, 67, 334

General Catalogue of Variable Stars. 1995, Vol. V, ed.-in chief N. N. Samus (Moscow, Kosmosiform)

Hernandez, X., Valls-Gabaud, D., & Gilmore, G. 1998, MNRAS, in press

Holtzman, J., Burrows, C., Casertano, S., Hester, J., Trauger, J., Watson, A., & Worthey, G. 1995, PASP, 107, 1065

Hunter, D., Baum, W., O'Neil Jr., E., & Lynds, R. 1996, ApJ, 468, 633 (HBOL)

Issa, M., MacLaren, I., & Wolfendale, A. 1990, A&A, 236, 237

Ivanov, G. 1996, A&A, 305, 708

_____. 1998, A&A, 337, 39

Langer, N., & Maeder, A. 1995, A&A, 295, 685

Magnier, E., Prins, S., Augustejn, T., van Paradijs, J., & Lewin, W. 1997, A&A, 326, 442

Massey, P. 1998, ApJ, 501, 153

Massey, P., Armandroff, T., & Conti, P. 1986, AJ, 92, 1303 (MAC)

Massey, P., Armandroff, T., Pyke, R., Patel, K., & Wilson, C. 1995, AJ, 110, 2715

Odewahn, S. 1987, AJ, 93, 310

Ratnatunga, K., & Bahcall, J. 1985, ApJS, 59, 63

Schaerer, D., Charbonnel, C., Meynet, G., Maeder, A., & Schaller, G. 1993, A&AS, 102, 339

Straizys, V. 1977, in Multicolor Stellar Photometry (Vilnius: Mokslas Publishers, in Russian), 105

Tosi, M., Greggio, L., Marconi, G., & Focardi, P. 1991, AJ, 102, 951

Valentijn, E. 1990, Nature, 346, 153

van den Bergh, S. 1964, ApJS, 9, 65

G. R. Ivanov and Petko Nedialkov: Department of Astronomy, University of Sofia, 5 James Bourchier Blvd., Sofia 1126, Bulgaria   (ivanov,japet@phys.uni-sofia.bg).

Todor Veltchev: Institute of Astronomy, Bulgarian Academy of Sciences, 72 Tsarigradsko Chausse Blvd., Sofia 1784, Bulgaria   (eirene@phys.uni-sofia.bg).